ChemComm

View Online
Dynamic Article Links

Cite this: *Chem. Commun.*, 2011, **47**, 11492–11494

www.rsc.org/chemcomm

COMMUNICATION

Polymorphic porous supramolecular networks mediated by halogen bonds on Ag(111)†

Kyung-Hoon Chung,[a] Jihun Park,[a] Kye Yeop Kim,[b] Jong Keon Yoon,[a] Howon Kim,[a] Seungwu Han*[b] and Se-Jong Kahng*[a]

Received 29th July 2011, Accepted 14th September 2011
DOI: 10.1039/c1cc14679c

Intermolecular structures of porous two-dimensional supramolecular networks are studied using scanning tunnelling microscopy combined with density functional theory calculations. The local configurations of halogen bonds in polymorphic porous supramolecular networks are directly visualized in support of previous bulk crystal studies.

Porous supramolecular networks have attracted much attention due to their possible applications including gas storage, heterogeneous catalysis, information storage, and in sensor devices.[1] They can be fabricated by molecular self-assembly mechanisms in which molecules themselves find specific locations that are stabilized by energy gains of intermolecular bonds.[2] On metal surfaces, well-ordered porous structures including rectangular, ladder, honeycomb, Kagome, chevron, and flower-like networks were fabricated using different molecules, as observed in scanning tunneling microscopy (STM) studies.[3,4] Electrostatic intermolecular interactions such as van der Waals, dipole–dipole, metal–ligand, and hydrogen bonds were used in these structures.[5] It was recently demonstrated using STM that supramolecular networks were mediated by halogen bonds, between two covalently bonded halogen atoms, or between a covalently bonded halogen and a donor atom such as O or N.[6–9] Such halogen bonds are made possible by unusual charge distributions that have both positive and negative parts in covalently-bonded halogen atoms.[10,11]

It has been suggested that molecular crystals with porous two-dimensional (2-D) honeycomb layers mediated by halogen bonds could be grown in solution phases by mixing a tridentate molecule with a rod-like molecule or with another tridentate molecule.[10] However, such halogen bonded porous structures have been rarely studied with STM combined with density functional theory (DFT) calculations that is powerful to reveal the detailed molecular configurations. In this study, we used a rod-like molecule, 4,4′′-dibromo-*p*-terphenyl (DBTP), to fabricate porous 2-D networks and visualize them using STM on Ag(111). We observed polymorphic network structures made of square, rectangular, and hexagonal pores. The molecules were self-assembled by means of triangular motifs with a Br···Br bond and a Br···H bond. We propose and reproduced molecular models for the observed structures using DFT calculations with van der Waals correction. The geometry of intermolecular bonds formed in the Br-terminated DBTP molecule was in a stark contrast to the geometries formed in a CN-terminated rod-like molecule.[4,12]

The chemical structure and calculated electrostatic potential of a DBTP molecule are shown in Fig. 1(a) and (b), respectively. The unique potential distribution around the Br atoms underlies the physical origin of halogen bonds.[10,11] Fig. 1(c) describes a possible bond configuration between two DBTP molecules that are overlaid by schematic electrostatic potentials deduced from Fig. 1(b). Since Br has both positive and negative electrostatic parts, it can be attracted by negative Br as well as positive H. Therefore, the two molecules are doubly bonded by Br···Br and Br···H pairs, as indicated by dotted lines in Fig. 1(c), resulting in a triangular motif. In network structures, four (three) molecules can combine to form the quartet (triplet) nodes of windmill shapes based on the triangular motifs.

Figure 2 shows STM images and corresponding molecular models for three different structures (square, rectangular, and

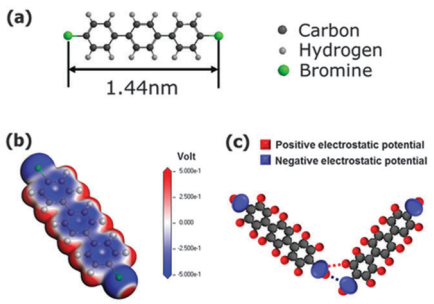

Fig. 1 (a) Chemical structure of the 4,4′′-dibromo-*p*-terphenyl (DBTP) molecule. (b) The calculated molecular electrostatic potential distribution of the DBTP molecule at the isodensity surface shown in red (positive) and blue (negative). (c) Schematic for two DBTP molecules with simplified electrostatic potential distributions around H and Br atoms. Dotted lines indicate possible intermolecular bonds, Br···Br (blue) and Br···H (red).

[a] *Department of Physics, Korea University, 1-5 Anam-dong, Seongbuk-gu, 136-713, Seoul, Korea. E-mail: sjkahng@korea.ac.kr; Fax: +82 2922 3484; Tel: +82 23290 3599*
[b] *Department of Materials Science and Engineering, Seoul National University, Seoul 151-744, Korea. E-mail: hansw@snu.ac.kr; Fax: +82 2 883 8197; Tel: +82 2 880 1541*

† Electronic supplementary information (ESI) available. See DOI: 10.1039/c1cc14679c

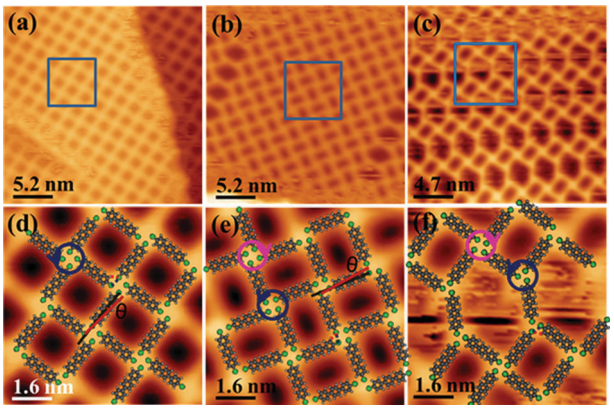

Fig. 2 (a)–(c) STM topography images of three porous networks obtained after a DBTP molecule was deposited on Ag(111) at 80 K. (d)–(f) High resolution STM images from the square marked areas of (a), (b), (c), respectively, which are superimposed with molecular models. Sizes of STM images: (a) 26 × 26 nm^2, (b) 26 × 26 nm^2, (c) 23.5 × 23.5 nm^2, and (d)–(f) 8 × 8 nm^2. For all images, tunneling current I_T = 0.1 nA and sample voltage V_S = 1 V.

hexagonal networks) formed on Ag(111) at 150 K. First, we discuss on the molecular configurations of the square and the rectangular networks. In both networks, a quartet node forms with four DBTP molecules connected by four triangular motifs discussed above. Therefore, the joint mechanism would be identical between these two network structures. The difference between the square and the rectangular network lies in the chiral structures; the quartet windmill nodes exhibit structural chirality even if the molecules themselves are achiral. The square network has only one type of chiral direction within a domain, whereas the rectangular network has both types of chiral directions that alternate between neighbouring nodes.

Next, we consider the molecular configurations of the hexagonal network. Hexagons have row structures. Two hexagon rows are separated by a rectangle row. The node structures of rectangles in a row are intrinsically the same as those in rectangular networks: they have four quartet windmill nodes. Two of them are shared by hexagons. Thus, a hexagon has two 90° and four 135° angles. At the nodes of 135°, triplet windmill nodes form. We expected that a triplet windmill was made from three Br···Br and three Br···H bonds. However, two Br···H bonds were missing, which we will describe subsequently. The chiral directions between two neighboring nodes in hexagon structures are the same (the opposite) if they are along (perpendicular to) the direction of a hexagon row.

Hexagon structures with co-existing triplet and quartet nodes are reminiscent of hydrogen bonded flower networks in trimesic acid.[13] Inner parts of hexagons were fuzzy, different from those of rectangles. A hexagon has a large enough area to encage a DBTP molecule that keeps moving due to thermal energy at 80 K. The porous area of a hexagon (8.39 nm^2) is larger than twice the area of a square (3.61 nm^2) and a rectangle (3.52 nm^2). Three structures were observed at lower temperatures down to 20 K without any other structure or disordered region. At room temperature, chain structures were observed due to cleavage of C–Br bonds, which will be discussed elsewhere.[15]

We performed DFT calculations and confirmed the models inferred by experiment as shown in Fig. 3. The equilibrium lattice distances of square and rectangular networks were 1.98 nm and 2.75 nm, and the lattice distances of hexagonal networks along two perpendicular directions were 2.82 nm and 4.58 nm, in excellent agreement with experimental observations (1.97 ± 0.05 nm, 2.74 ± 0.05 nm, 2.83 ± 0.05 nm, and 4.60 ± 0.05 nm, respectively). The angles in the hexagons were 90° and 135°. In the nodes of the squares and rectangles, the long axes of two molecules formed 90° angles, and two Br···Br bonds also formed 90° angles. However, the long axis of a molecule and Br···Br bonds are not parallel; rather, they have 7.6° and 6.9° angles in the square and the rectangular networks, respectively, as noted by θ in Fig. 3(a) and (b). This is also in good agreement with the experimental models shown in Fig. 2 (8 ± 1° and 7 ± 1°). These structural features are a result of competition between Br···Br and Br···H bonds.[16] While Br···H bonds tend to increase the tilt angle θ, Br···Br bonds are more stable when in parallel with the molecular axis. The bond distances computed from the theoretical equilibrium structures are summarized in the ESI†, they imply that Br···Br and Br···H are reasonable entities of the porous networks.[16] We notice that the two distances between Br and H atoms in the triplet windmill are 0.40 nm and 0.48 nm, which are too large to be bonds.

The net energy gains for the square, rectangular, and hexagonal structures were 220 meV, 220 meV, and 160 meV per molecule, respectively, as shown in Fig. 3(d)–(f). In bulk cases, we estimated that the strengths (distances) of the Br···H and Br···Br bonds under similar molecular environments (covalently bonded to C atoms) were about 70 meV (0.30 nm) and 60 meV (0.38 nm), respectively.[18] Based on these bond strengths, the energy gains of the systems can be estimated by counting the number of intermolecular bonds per molecule. In both the square and rectangular networks, a DBTP molecule has 2 Br···Br and 2 Br···H bonds. In a hexagonal network, a DBTP molecule has 2 Br···Br and 1.2 Br···H bonds. Therefore, the expected energy gains for square, rectangular, and

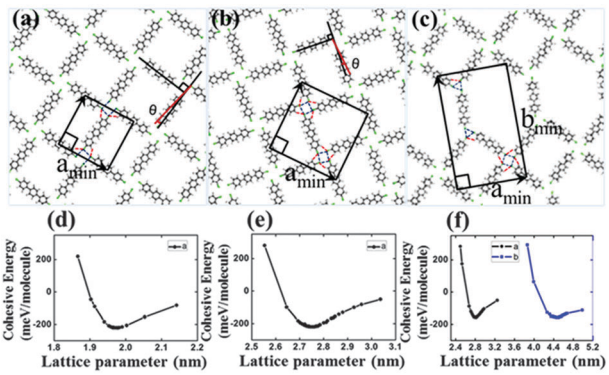

Fig. 3 The calculated atomic structures (a) square, (b) rectangular, and (c) hexagonal structures and the energy gains per molecule as a function of lattice parameters for the (d) square, (e) rectangular, and (f) hexagonal structures. The 2-D unit cell vectors and possible intermolecular interactions are drawn with solid and dotted lines, respectively in (a), (b), and (c). The computed energy is shown in (d), (e), and (f). For the hexagonal structure, only two graphs are displayed for simplicity with a fixed angle and ratio between a and b, although we performed calculations by considering each of them as an independent variable.

hexagonal networks are 260 meV, 260 meV, and 200 meV per molecule, respectively. The preceding computational results were about 40 meV lower than this rough estimation. Some part of the discrepancy may be related to limitations of density functional theory such as the inability to describe dispersion interactions accurately. (We considered the dispersion interactions by semiempirical methods (see ESI†).)

The calculation results indicate that the square and rectangular networks were more favourable than the hexagonal network. However in our STM experiments, the hexagonal network occupied about 70% of the total scanned area. (Rectangular and square networks were 20% and 10%, respectively.) In the calculations, the substrate was not taken into account. The hexagonal structures may have had more energy gains than others when molecules formed their structures on the hexagonal atomic lattices of Ag(111).[18] To achieve a better understanding of our results, substrate effect should be considered in the calculations.

In conclusion, we studied the porous supramolecular networks of DBTP on Ag(111) using STM. Three different molecular structures—square, rectangular, and hexagonal—were observed. Based on STM images, we proposed molecular models that are in good agreement with DFT studies, and can be explained using a triangular motif consisting of a Br···Br and a Br···H bond. The measured bonding distances and strengths are consistent with existing bulk data. Although we performed experiments at low-temperature, halogen bonds are active at room temperature in other systems.[8–10] We envision that the dimensions of these porous structures can be scaled up by increasing the lengths of the molecules preserving the Br termination. The observed structures can be used to create porous supramolecular structures in various forms.

The authors gratefully acknowledge financial support from National Research Foundation of Korea, funded by the Ministry of Education, Science and Technology of the Korean government (grant nos. 2005-2002369, 2007-0054038). KYK and SH were supported by Basic Science Research Program (2010-0011085).

Notes and references

1 (*a*) R. B. Wehrspohn, *Ordered Porous Nanostructures and Applications*, Springer, 2011; (*b*) C. N. R. Rao, S. Natarajan and R. Vaidhyanathan, *Angew. Chem., Int. Ed.*, 2004, **43**, 1466–1496; (*c*) N. Z. Logar and V. Kaučič, *Acta Chim. Slov.*, 2006, **53**, 117–135; (*d*) J. A. A. W. Elemans, S. Lei and S. De Feyter, *Angew. Chem., Int. Ed.*, 2009, **48**, 7298–7332.

2 (*a*) K. J. M. Bishop, C. E. Wilmer, S. Soh and B. A. Grzybowski, *Small*, 2009, **5**, 1600–1630; (*b*) J. V. Barth, G. Costantini and K. Kern, *Nature*, 2005, **437**, 671–679.

3 (*a*) S. L. Tait, A. Langner, N. Lin, R. Chandrasekar, O. Fuhr, M. Ruben and K. Kern, *ChemPhysChem*, 2008, **9**, 2495–2499; (*b*) S. Stepanow, M. Lingenfelder, A. Dmitriev, H. Spillmann, E. Delvigne, N. Lin, X. Deng, C. Cai, J. V. Barth and K. Kern, *Nat. Mater.*, 2004, **3**, 229–233; (*c*) G. Pawin, K. L. Wong, K.-Y. Kwon and L. Bartels, *Science*, 2006, **313**, 961–962; (*d*) L. Kampschulte, M. Lackinger, A.-K. Maier, R. S. K. Kishore, S. Griessl, M. Schmittel and W. M. Heckl, *J. Phys. Chem. B*, 2006, **110**, 10829–10836; (*e*) S. Lei, M. Surin, K. Tahara, J. Adisoejoso, R. Lazzaroni, Y. Tobe and S. De Feyter, *Nano Lett.*, 2008, **8**, 2541–2546; (*f*) S. Lei, K. Tahara, X. Feng, S. Furukawa, F. C. De Schryver, K. Müllen, Y. Tobe and S. De Feyter, *J. Am. Chem. Soc.*, 2008, **130**, 7119–7129.

4 (*a*) F. Klappenberger, D. Kühne, W. Krenner, I. Silanes, A. Arnau, F. J. García de Abajo, S. Klyatskaya, M. Ruben and J. V. Barth, *Nano Lett.*, 2009, **9**, 3509–3514; (*b*) U. Schlickum, R. Decker, F. Klappenberger, G. Zoppellaro, S. Klyatskaya, W. Auwarter, S. Neppl, K. Kern, H. Brune, M. Ruben and J. V. Barth, *J. Am. Chem. Soc.*, 2008, **130**, 11778–11782.

5 (*a*) O. Guillermet, E. Niemi, S. Nagarajan, X. Bouju, D. Martrou, A. Gourdon and S. Gauthier, *Angew. Chem., Int. Ed.*, 2009, **48**, 1970–1973; (*b*) H. Dil, J. Lobo-Checa, R. Laskowski, P. Blaha, S. Berner, J. Osterwalder and T. Greber, *Science*, 2008, **319**, 1824–1826; (*c*) D. Heim, K. Seufert, W. Auwärter, C. Aurisicchio, C. Fabbro, D. Bonifazi and J. V. Barth, *Nano Lett.*, 2010, **10**, 122–128; (*d*) J. A. Theobald, N. S. Oxtoby, M. A. Phillips, N. R. Champness and P. H. Beton, *Nature*, 2003, **424**, 1029–1031; (*e*) R. Otero, M. Lukas, R. E. A. Kelly, W. Xu, E. Lægsgaard, I. Stensgaard, L. N. Kantorovich and F. Besenbacher, *Science*, 2008, **319**, 312–315.

6 H. Walch, R. Gutzler, T. Sirtl, G. Eder and M. Lackinger, *J. Phys. Chem. C*, 2010, **114**, 12604–12609.

7 (*a*) J. K. Yoon, W.-j. Son, K.-H. Chung, H. Kim, S. Han and S.-J. Kahng, *J. Phys. Chem. C*, 2011, **115**, 2297–2301; (*b*) J. K. Yoon, W.-j. Son, H. Kim, K.-H. Chung, S. Han and S.-J. Kahng, *Nanotechnology*, 2011, **22**, 275705.

8 J. C. Russell, M. O. Blunt, J. M. Garfitt, D. J. Scurr, M. Alexander, N. R. Champness and P. H. Beton, *J. Am. Chem. Soc.*, 2011, **133**, 4220–4223.

9 R. Gutzler, O. Ivasenko, Ch. Fu, J. L. Brusso, F. Rosei and D. F. Perepichka, *Chem. Commun.*, 2011, **47**, 9453–9455.

10 P. Metrangolo, F. Meyer, T. Pilati, G. Resnati and G. Terraneo, *Angew. Chem., Int. Ed.*, 2008, **47**, 6114–6127.

11 (*a*) O. Hassel, *Science*, 1970, **170**, 497–502; (*b*) G. R. Desiraju and R. Parthasarathy, *J. Am. Chem. Soc.*, 1989, **111**, 8725–8726.

12 D. Kühne, F. Klappenberger, R. Decker, U. Schlickum, H. Brune, S. Klyatskaya, M. Ruben and J. V. Barth, *J. Phys. Chem. C*, 2009, **113**, 17851–17859.

13 S. Griessl, M. Lackinger, M. Edelwirth, M. Hietschold and W. M. Heckl, *Single Mol.*, 2002, **3**(1), 25–31.

14 K.-H. Chung, H. Kim, J. K. Yoon and S.-J. Kahng, unpublished.

15 (*a*) C. B. Aakeröy, M. Fasulo, N. Schultheiss, J. Desper and C. Moore, *J. Am. Chem. Soc.*, 2007, **129**, 13772–13773; (*b*) P. Politzer, J. S. Murray and P. Lane, *Int. J. Quantum Chem.*, 2007, **107**, 3046–3052.

16 (*a*) R. S. Rowland and R. Taylor, *J. Phys. Chem.*, 1996, **100**, 7384–7391; (*b*) F. Neve and A. Crispini, *Cryst. Growth Des.*, 2001, **1**, 387–393; (*c*) V. Rajnikant, D. Jasrotia and B. Chand, *J. Chem. Crystallogr.*, 2008, **38**, 211–230.

17 (*a*) F. F. Awwadi, R. D. Willett, K. A. Peterson and B. Twamley, *Chem.–Eur. J.*, 2006, **12**, 8952–8960; (*b*) A. Kovács and Z. Varga, *Coord. Chem. Rev.*, 2006, **250**, 710–727; (*c*) Y. Futami, S. Kudoh, F. Ito, T. Nakanaga and M. Nakata, *J. Mol. Struct.*, 2004, **690**, 9–16; (*d*) J. Xu, W.-L. Wang, T. Lin, Z. Sun and Y.-H. Lai, *Supramol. Chem.*, 2008, **20**, 723–730.

18 L. M. A. Perdigão, P. A. Staniec, N. R. Champness, R.E. A. Kelly, L. N. Kantorovich and P. H. Beton, *Phys. Rev. B: Condens. Matter Mater. Phys.*, 2006, **73**, 195423.

